Interaction of fast charged projectiles with two-dimensional electron gas: Interaction and collisional-damping effects

Hrachya B. Nersisyan[1,2,*] and Amal K. Das[3,†]
[1]*Division of Theoretical Physics, Institute of Radiophysics and Electronics, Alikhanian Brothers Street 1, 378410 Ashtarak, Armenia*
[2]*Centre of Strong Fields Physics, Yerevan State University, Alex Manoogian Street 1, 375025 Yerevan, Armenia*
[3]*Department of Physics, Dalhousie University, Halifax, Nova Scotia, Canada B3H 3J5*
(Received 15 January 2009; published 10 July 2009)

The results of a theoretical investigation on the stopping power of ions moving in a two-dimensional degenerate electron gas are presented. The stopping power for an ion is calculated employing linear-response theory using the dielectric function approach. The collisions, which lead to a damping of plasmons and quasiparticles in the electron gas, is taken into account through a relaxation-time approximation in the linear-response function. The stopping power for an ion is calculated in both the low- and high-velocity limits. In order to highlight the effects of damping, we present a comparison of our analytical and numerical results, in the case of pointlike ions, obtained for a nonzero damping with those for a vanishing damping. It is shown that the equipartition sum rule first formulated by Lindhard and Winther for three-dimensional degenerate electron gas does not necessarily hold in two dimensions. We have generalized this rule introducing an effective dielectric function. In addition, some results for two-dimensional interacting electron gas have been obtained. In this case, the exchange-correlation interactions of electrons are considered via local-field corrected dielectric function.

DOI: 10.1103/PhysRevE.80.016402 PACS number(s): 52.40.Mj, 52.25.Mq, 73.50.Mx, 52.27.Gr

I. INTRODUCTION

There is an ongoing interest in the theory of interaction of swift charged projectiles with condensed matter. Although most theoretical works have reported on the energy loss of ions in a target medium which is modeled as a three-dimensional (3D) electron gas, the two-dimensional (2D) case has not yet received as much attention as the 3D case. A 2D electron system is now experimentally realizable in a laboratory. In the last 3 decades or so, many interesting and intriguing properties of a 2D electron gas have been explored. For a recent update on some of these developments, we refer to Refs. [1,2]. A widely used 2D electron system is realized at the interface between GaAs and $Ga_{1-x}Al_xAs$ and in the interface metal-oxide semiconductors. The interaction of charged particles with an electron gas is an important probe of many-body interactions in the target electron medium. It is known that many-body properties of an electron gas vary in notable aspects with spatial dimensions. It is therefore of interest to make a detailed study of interaction of charged particles with a 2D electron gas. This theoretical study is also of relevance to device applications, e.g., in using ion implantation in devices which involve 2D electron systems.

In general, interaction of charged projectiles with condensed matter can be studied by means of the stopping power (SP) of the target medium. The SP accounts for the energy loss by an external charged projectile as it passes through and interacts with matter. Moreover, the SP of a medium can be used to construct diagnostic tools for studying this kind of physical systems. There have been several theoretical approaches to the energy loss and SP for 3D systems and some of these approaches have been applied also to a 2D electron gas. Among previous theoretical works on a 2D electron gas, some are based on the linear-response dielectric function method [3–9] and quantum-scattering theory [10–13]. Further works have dealt with some nonlinear screening effects through a quadratic response approach within the random-phase approximation [14], the employment of density-functional theory [15], and, more recently, in a method based on frequency moments of the energy loss function [8,9].

In this paper, we shall consider fast charged projectiles and hence a linear-response theory to calculate energy loss is expected to be adequate. Previously, within this approach, Bret and Deutsch calculated the SP of an ion [3,4] and a dicluster [5] in a 2D electron gas for any degeneracy. Their results show some interesting differences with the corresponding results for a 3D case. Of special interest is their finding that the leading term of the asymptotic expansion of the SP in a high-velocity limit decreases as $1/v$, where v is the projectile velocity, which differs from the well-known form predicted by the Bethe-Bloch formula [16–18] in the 3D case. The calculations in Refs. [3–5] are based on the random-phase approximation (RPA) which works well if electron-electron interaction can be neglected. Now, in 2D systems, electron density can be varied. For moderate values of electron density, e.g., in semiconductors, electron-electron interaction may not be negligible and going beyond RPA is desirable.

Our objective is to consider two physically motivated aspects of a 2D electron gas in the context of energy loss. For the first part of our study, we consider an electron gas taking into account the collisional damping. The effect of the damping is included through a phenomenological relaxation time for electrons due to scattering by impurities, phonons, elec-

*hrachya@irphe.am
†akdas@dal.ca

trons, etc. For this system, we use a linear-response dielectric function in RPA and in a number-conserving relaxation-time approximation (RTA), which was first considered by Mermin [19] and then by Das [20] for a 3D electron gas. This RTA formulation has not yet been extended beyond RPA. The effect of the collisions which leads to a damping of excitations enters the RPA dielectric function, for a given collision frequency, through $\varepsilon_{\mathrm{RPA}}(k,\omega+i\gamma)$, where γ is used as a model parameter. For a degenerate electron gas (DEG) and for a given electron density, the damping parameter can be assumed to be a constant to a good approximation. The damping-inclusive dielectric function, with the collision frequency as a free parameter, allows some physical insights and useful numerical estimates of the influence of the collisions on energy loss in a DEG. In 3D, the predicted effect is a shorter lifetime with a smaller propagation wavelength of plasmons resulting considerable modifications of the SP (see, e.g., Refs. [21–25] and references therein). For the stopping of a single ion, the broadening of the plasmon peak with increasing γ shifts the threshold for energy loss by plasmon excitation toward lower projectile velocities. It now becomes possible for low-velocity projectile ions to excite plasmons (in addition to single-particle excitations). This increases the SP of 3D electron gas at low projectile velocities, compared to the damping-free RPA result [23–25]. The situation with a 2D electron gas will be discussed in detail in the following sections.

The second objective of our study is to investigate the influence of exchange-correlation interaction (i.e., beyond RPA) in an electron gas on the SP. For a 3D electron system, it has been shown [26,27] that the SP in low- and intermediate-velocity regimes shows a definite increase due to this interaction. A similar result has been reported for a 2D system [6,7]. However, let us note that if an asymptotic expansion of the SP in a high-velocity regime is considered then it has been shown previously in Refs. [8,9] that the first term in this expansion is unaffected by electron-electron interaction. In this paper, we calculate the next nonvanishing term of this asymptotic expansion and show that it behaves as $B(r_s)v^{-4}\ln[A(r_s)v]$, where exchange-correlation interactions are involved in $A(r_s)$ and $B(r_s)$. These functions depend on the target density through Wigner-Seitz density parameter $r_s=(\pi n_0 a_0^2)^{-1/2}$, where n_0 and a_0 are electron gas density and Bohr radius, respectively. The details are presented in Sec. III.

The plan of the paper is as follows. In Sec. II A we derive analytical expressions for the damping-inclusive dielectric function (DF) for a 2D degenerate electron gas. We would like to mention that an alternative but equivalent derivation is presented in Appendix A. The latter derivation contains certain attractive features. Through this alternative formulation, we consider a small-k,ω approximation for the DF and this approximate result is used in Sec. II A. In a small-k,ω approximation, the plasmon dispersion for a two-dimensional DEG involving collisional damping exhibits a constraint not present in 3D. This behavior has been previously discussed in the literature [28–30]. We revisit this approximation through our formulation in Appendix A. The exact plasmon dispersion relations for an interacting DEG (including exchange-correlation effects) are derived in Sec. II B by employing local-field corrections to the RPA dielectric function. In Sec. III, we briefly outline the general linear-response function formalism of the 2D stopping power of a pointlike ion. After dealing with the excitation equipartition in Sec. III A, we develop, in Secs. III B and III C, some analytical techniques to calculate the SP of an ion in low- and high-velocity regimes. The two particular cases studied in these sections are (i) low-velocity limit of the SP for an ion moving in a damping-inclusive DEG and (ii) high-velocity limit for a strongly interacting DEG. Section IV contains some numerical examples for the SP. The results are summarized in Sec. V which also includes discussion and outlook. Appendix A, to which we draw the reader's attention, presents the above-mentioned alternative derivation of the DF for the damping-inclusive case in RPA, which is also valid in the complex ω plane. In Appendix B, we provide some technical details for an evaluation of the asymptotic SP.

II. DIELECTRIC FUNCTION AND DISPERSION RELATIONS FOR 2D ELECTRON GAS

In the linear-response theory, the SP of an external projectile moving in a medium is related to the dielectric function $\varepsilon(k,\omega)$ of the medium. Both the single-particle and collective excitations (i.e., the plasmons) contribute to the SP and these contributions are contained in $\varepsilon(k,\omega)$. In our study, the 2D target medium is assumed to contain the damping effects due to the collisions of electrons with impurities, etc. We shall incorporate effects of the collisional damping in $\varepsilon(k,\omega)$ in a somewhat phenomenological manner. This is to include the damping through a relaxation time τ such that the particle number is conserved. For a 3D medium, this was done first by Mermin [19] and then by Das [20] in the RPA and in RTA. We refer the reader to [19,20] for details of this formalism. For $\tau\to\infty$, this linear-response function $\varepsilon(k,\omega,1/\tau)$ reduces to the Lindhard dielectric function [17,18]. The dielectric function $\varepsilon(k,\omega)$ is understood to contain $\gamma=1/\tau$ as a damping parameter. The form of $\varepsilon(k,\omega,1/\tau)$ is to be specified shortly for a 2D electron gas.

It is convenient to introduce the dimensionless Lindhard variables $z=k/2k_F$, $u=\omega/kv_F$, where v_F and $k_F=(2\pi n_0)^{1/2}$ are, respectively, the Fermi velocity and wave number of the target electrons. Also we introduce the density parameters $\chi^2=1/\alpha=1/k_F a_0=r_s/\sqrt{2}$. In our calculations, χ and α (or r_s) serve as a measure of electron density. (Note that the density parameter χ introduced above differs from usual definition by a factor π, see, e.g., Refs. [3–6]).

A. Collisional damping in RPA

Let us now specify the damping-inclusive dielectric function for 2D zero-temperature (degenerate) electron gas. This has been done previously in Refs. [28–30] employing small-k,ω approximation. Here within RPA and RTA, we derive the damping-inclusive DF without further approximations on the energy-momentum spectrum, i.e., on ω and k. As pointed out in Ref. [29], the physical arguments for deriving number-conserving DF by Mermin [19] and Das [20] in 3D are independent of dimensionality. Therefore, with the nota-

tions introduced in the preceding paragraph, the DF for 2D DEG reads

$$\varepsilon(z,u) = 1 + \frac{(zu+i\Gamma)[\varepsilon_{\mathrm{RPA}}(z,u,\Gamma)-1]}{zu+i\Gamma[\varepsilon_{\mathrm{RPA}}(z,u,\Gamma)-1]/[\varepsilon_{\mathrm{RPA}}(z,0)-1]}, \tag{1}$$

where $\Gamma=\hbar\gamma/4E_F$, $E_F=\hbar^2k_F^2/2m$ being the Fermi energy with m as the effective mass. The quantity γ (or Γ) is a measure of collisional damping of excitations in the electron gas. $\varepsilon_{\mathrm{RPA}}(z,u,\Gamma)=\varepsilon_{\mathrm{RPA}}(k,\omega+i\gamma)$ is the longitudinal dielectric function of DEG in the RPA derived in 2D by Stern [31]. $\varepsilon_{\mathrm{RPA}}(z,0)=\varepsilon_{\mathrm{RPA}}(k,0)$ is the static dielectric function. We have analytically evaluated the damping-inclusive $\varepsilon(z,u)$ for which the results, presented below, appear to be new and we have utilized them in our numerical examples.

It should be emphasized that for realistic systems, there are a number of physical mechanisms such as collisions with impurities (disorder), phonons, etc., which contribute to the damping parameter γ (see, e.g., Refs. [32,33] and references therein). Moreover, contribution of each mechanism depends strongly on the specific conditions of the material. We have not attempted here to evaluate the damping parameter from first principles but have regarded it as a model parameter. In principle, γ can be calculated to varying degrees of approximations. In the simplest approximation, its inverse can be calculated through Fermi's golden rule for a model electron-impurity potential. This may allow us to see how SP and related quantities depend on the target properties through their influence on γ. Alternatively, the model relaxation time τ can be estimated from the experimental data of the dc conductivity or the mobility in 2D systems. Using the data given, for instance, in Refs. [32,33] (see also [28]), we have found that in 2D systems, the typical values of the damping parameter vary (in terms of the Fermi energy) in the domain $\hbar\gamma/E_F \lesssim 0.3$ ($\Gamma \lesssim 0.1$).

Let us recall the Lindhard (RPA) expression for the longitudinal dielectric function [17]. In variables z and u and in 2D, it reads as [31]

$$\varepsilon_{\mathrm{RPA}}(z,u,\Gamma) = 1 + \frac{\chi^2 z}{\pi}\int_0^\pi d\theta \int_0^1 \frac{qdq}{z^4-(uz+i\Gamma+qz\cos\theta)^2}$$
$$= 1 + \frac{\chi^2}{2z^2}[F_1(z,u,\Gamma)+iF_2(z,u,\Gamma)], \tag{2}$$

where we have split explicitly the DF $\varepsilon_{\mathrm{RPA}}(z,u,\Gamma)$ into the real and imaginary parts and have introduced the real functions (for real z and u) $F_1(z,u,\Gamma)$ and $F_2(z,u,\Gamma)$ as in the usual RPA expression of longitudinal dielectric function.

Performing the q and θ integrations in Eq. (2) [34], we obtain, for a nonzero damping,

$$F_1(z,u,\Gamma) = 2z + \frac{\Gamma}{z}[Y_-(z,u_-)-Y_-(z,u_+)] + (u_- - 1)Y_+(z,u_-)$$
$$-(u_+-1)Y_+(z,u_+), \tag{3}$$

$$F_2(z,u,\Gamma) = \frac{\Gamma}{z}[Y_+(z,u_-)-Y_+(z,u_+)] + (u_+-1)Y_-(z,u_+)$$
$$-(u_- - 1)Y_-(z,u_-), \tag{4}$$

with $u_\pm = u \pm z$,

$$Y_\pm(z,u) = \frac{1}{\sqrt{2}}\sqrt{\sqrt{\frac{z^2(u+1)^2+\Gamma^2}{z^2(u-1)^2+\Gamma^2}} \pm \frac{z^2(u^2-1)+\Gamma^2}{z^2(u-1)^2+\Gamma^2}}. \tag{5}$$

In the case of vanishing damping ($\gamma\to 0$ and $\Gamma\to 0$), the expressions (1)–(5) coincide with the Stern result [31] with

$$f_1(z,u) = F_1(z,u,0) = 2z + C_-\sqrt{u_-^2-1} - C_+\sqrt{u_+^2-1}, \tag{6}$$

$$f_2(z,u) = F_2(z,u,0) = D_-\sqrt{1-u_-^2} - D_+\sqrt{1-u_+^2}, \tag{7}$$

$$D_\pm = H(1-|u_\pm|), \quad C_\pm = H(|u_\pm|-1)\frac{u_\pm}{|u_\pm|}. \tag{8}$$

Here, $H(z)$ is the Heaviside unit-step function. The static DF involved in Eq. (1) can be found either from Eqs. (3) and (4) at the limits $u\to 0$, $\Gamma\to 0$ or from Eqs. (6)–(8) at $u\to 0$. The result reads

$$\varepsilon_{\mathrm{RPA}}(z,0) = 1 + \frac{\chi^2}{z^2}f(z), \tag{9}$$

with

$$f(z) = \frac{1}{2}f_1(z,0) = \begin{cases} z, & 0\le z\le 1 \\ \dfrac{1}{z+\sqrt{z^2-1}}, & z>1. \end{cases} \tag{10}$$

To demonstrate the effect of the damping in Fig. 1, we show the contour plots of the energy loss function $L(z,u)=\mathrm{Im}[-1/\varepsilon(z,u)]$ without (left panel) and with (right panel) damping. The plasmon dispersion function $u_r(z)$ in the left panel is also shown as a dashed line (the explicit derivation of the plasmon dispersion curve $u_r(z)$ without damping is given below in Sec. II B, see Eqs. (16) and (19) and Fig. 3). The single-particle excitation energies $\hbar\omega_{\mathrm{sp}}=|\hbar k v_F \pm \hbar^2k^2/2m|$ (or $u=|z\pm 1|$ in dimensionless units) are demonstrated as thick solid lines. As expected, the energy loss function $L(z,u)$ in the case of vanishing damping (left panel) is localized in the domains $0<u<1-z$, with $0<z<1$, $|z-1|<u<z+1$ as well as on the plasmon curve $u_r(z)$ where the function $L(z,u)$ behaves as a Dirac δ function and becomes infinity. In the case of nonzero damping (right panel), the energy loss function is broadened due to the damping and becomes nonzero also in the domains $u<|z-1|$ and $u>z+1$.

Equations (1)–(4) constitute the number-conserving DF for a 2D electron gas involving the damping effects. Deriving these expressions, we have explicitly split the DF into real and imaginary parts assuming real variables z and u. An alternative (but equivalent) expression for this DF is derived in Appendix A which is valid for any complex ω and k. With this exact (within RPA and RTA) expression in Appendix A,

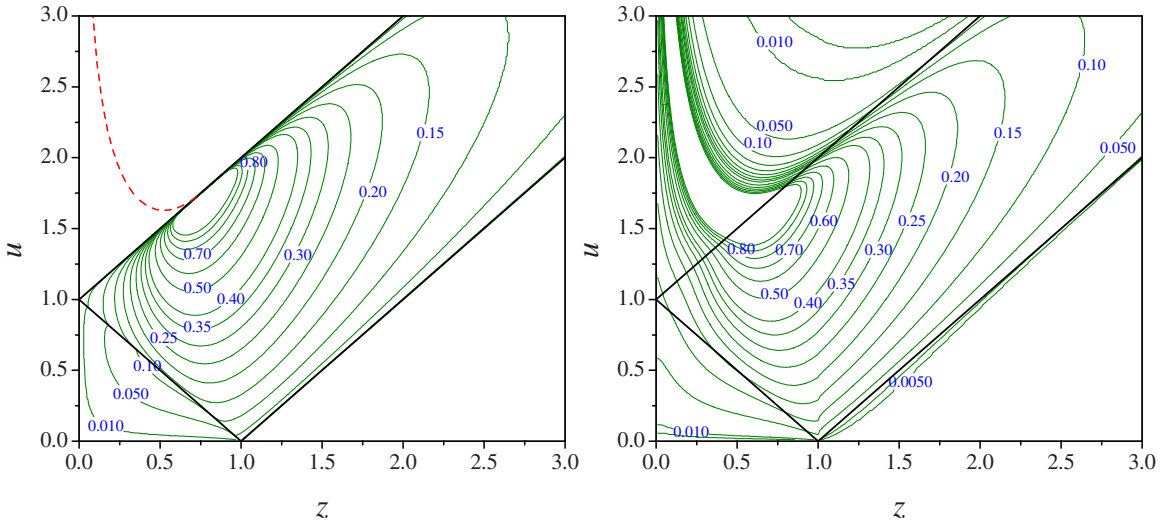

FIG. 1. (Color online) The contour plot of $L(z,u)=\mathrm{Im}[-1/\varepsilon(z,u)]$ as a function of the variables z and u for $r_s=2$ and without (left panel) and with (right panel) damping ($\Gamma=0.06$). Dashed line in left panel shows the plasmon dispersion curve $u_r(z)$ (see the text for details) with $\Gamma=0$. The numbers indicate the values of $L(z,u)$.

we then calculate the DF within small ω,k approximation obtained previously in Refs. [28–30] and revisited in Appendix A. The basic feature of this approximation is the prediction of the threshold condition for plasmon propagation which is absent in 3D (see, e.g., Ref. [23]). Indeed, the solution of the dispersion equation $\varepsilon(k,\omega)=0$, where $\varepsilon(k,\omega)$ is given by Eq. (A8), reads [28–30]

$$\omega_r(k)=\frac{1+k\lambda_{\mathrm{TF}}}{1+k\lambda_{\mathrm{TF}}/2}\left[-\frac{i\gamma}{2}+\sqrt{\omega_p^2(k)\left(1+\frac{k\lambda_{\mathrm{TF}}}{2}\right)-\frac{\gamma^2}{4}}\right], \tag{11}$$

where $\omega_p^2(k)=2\pi n_0 e^2 k/m$ is the plasma frequency for a 2D electron gas. The condition that $\omega_r(k)$ has a real part (for plasmon propagation) leads to $k>k_*$, where

$$k_*=k_{\mathrm{TF}}\left[\sqrt{1+\left(\frac{\gamma}{k_{\mathrm{TF}}v_F}\right)^2}-1\right], \tag{12}$$

with $k_{\mathrm{TF}}=1/\lambda_{\mathrm{TF}}=2/a_0$. Thus, within small ω,k approximation, collisions in 2D electronic systems considerably soften plasmons; they cannot propagate for $k<k_*$ and their dispersion relation is strongly altered relative to the collisionless case. However, since these results were obtained in small ω,k domain, one can expect some modifications for large momentum transfers at $k\gtrsim k_*$. As an example in Fig. 2, we demonstrate the real (left panel) and imaginary (right panel) parts of the solutions of the dispersion equations with approximate [Eq. (11)] and exact dielectric functions, Eqs. (A3)–(A6). For simplicity, we consider the case $k\leq 2k_F$ when the function Q in Eq. (A5) vanishes. Note that the condition $k>k_*$ together with the inequality $k\leq 2k_F$ requires that $\gamma/\omega_H<4r_s^{-2}\sqrt{1.414r_s+1}$, with $\omega_H=me^4/\hbar^3$. It is seen that the slope of the imaginary part of $\omega_r(k)$ (right panel) is dramatically changed at some values of k where the expression under square root in Eq. (11) changes the sign. For small ω,k approximation, this value of k is given by Eq. (12). As pointed out in Appendix A, the approximation (11) is valid when one neglects the single-particle energy $\hbar\omega_k=\hbar^2k^2/2m$ with respect to $\hbar kv_F$. Therefore, in general, we expect good agreement between approximate and exact $\omega_r(k)$ for small momentum k, as shown in Fig. 2. However, with increasing

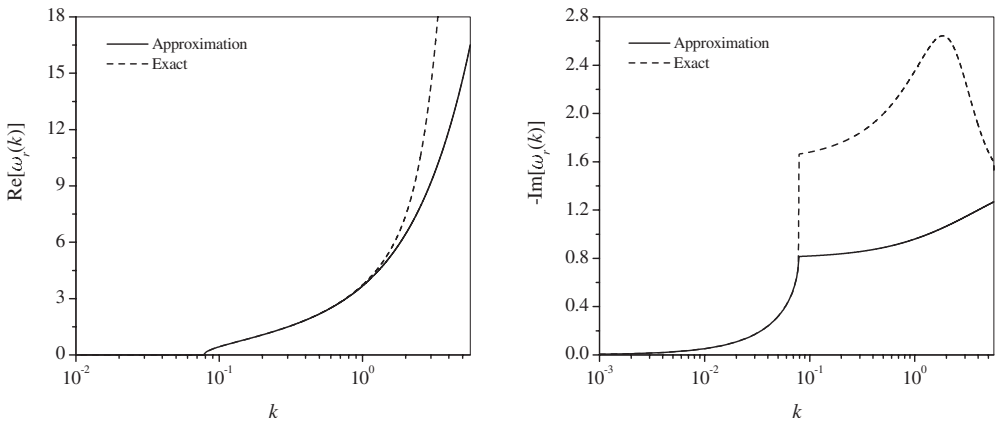

FIG. 2. Real ($\mathrm{Re}[\omega_r(k)]$, left panel) and imaginary ($\mathrm{Im}[\omega_r(k)]$, right panel) parts (in units of ω_{H}) of exact (dashed lines) and approximate (solid lines) solutions of dispersion equation vs k (in units of a_0^{-1}) for $k\leq 2k_F$, $r_s=0.5$, and $\Gamma=0.1$.

TABLE I. The critical wave numbers (dimensionless) z_c and the minimum values $\lambda_c=u_r(z_{\min})$ of the dispersion function $u_r(z)$ for some values of the density parameter r_s. $z_c^{(0)}$ and $\lambda_c^{(0)}$ represent the same quantities but for noninteracting 2D electron gas.

r_s	0.10	0.50	1.00	1.50	2.00	2.50	3.00	3.50	4.00
z_c	0.126	0.288	0.390	0.457	0.507	0.546	0.579	0.606	0.629
$z_c^{(0)}$	0.135	0.345	0.510	0.638	0.748	0.845	0.932	1.013	1.089
λ_c	1.116	1.264	1.358	1.421	1.469	1.507	1.538	1.565	1.588
$\lambda_c^{(0)}$	1.122	1.304	1.440	1.543	1.629	1.704	1.770	1.831	1.886

k, the approximate dispersion relation (11) fails to predict $\omega_r(k)$ correctly.

B. Strongly coupled electron gas: Beyond RPA

In this section, we consider exchange-correlation interaction effects via static local-field corrected (LFC) DF but we neglect the damping (i.e., $\gamma=0$). To include the damping in a fully interacting electron gas at a microscopic level is rather involved and no analytical calculations of $\varepsilon(k,\omega)$ without restrictions on k and ω are still available. An attempt to involve strong correlations in RTA and within small k,ω approximation [see Eq. (11)] has been done in Ref. [29]. Instead, we employ here the LFC dielectric function and demonstrate some useful results which have not been considered previously. Our discussion below is based on the static LFC dielectric function of a fully DEG, see, e.g., Ref. [6] (in dimensionless variables z and u)

$$\varepsilon(z,u) = 1 + \frac{\mathcal{P}(z,u)}{1 - G(z)\mathcal{P}(z,u)}, \tag{13}$$

where $\mathcal{P}(z,u)$ is the polarizability of the free-electron gas obtained in RPA by Stern [31]

$$\mathcal{P}(z,u) = \varepsilon_{\mathrm{RPA}}(z,u) - 1 = \frac{\chi^2}{2z^2}[f_1(z,u) + if_2(z,u)], \tag{14}$$

with $\varepsilon_{\mathrm{RPA}}(z,u)=\varepsilon_{\mathrm{RPA}}(z,u,\Gamma\to 0)$, where $\varepsilon_{\mathrm{RPA}}(z,u,\Gamma)$, $f_1(z,u)$, and $f_2(z,u)$ are given by Eqs. (2), (6), and (7), respectively. Note that our definition of the functions $f_1(z,u)$ and $f_2(z,u)$ differs from the definition given in Refs. [6,7] by a factor of $-1/2$. $G(z)$ is the static LFC function, which includes the effects of exchange-correlation interactions. Within a sum-rule version of the self-consistent approach, Gold and Calmels presented [35] a parameterized expression $G(z)$ for the 2D electron gas,

$$G(z) = \frac{zG_0(r_s)}{\sqrt{G_{12}^2(r_s) + z^2G_{22}^2(r_s)}}. \tag{15}$$

The coefficients $G_0(r_s)$, $G_{12}(r_s)$, and $G_{22}(r_s)$ are determined by $G_0(r_s)=1.983r_s^{1/3}$, $G_{12}(r_s)=1.626C_{12}(r_s)$, and $G_{22}(r_s)=\sqrt{2}r_s^{-1/3}C_{22}(r_s)$, with $C_{12}(r_s)=\alpha_1 r_s^{\gamma_1}$ and $C_{22}(r_s)=\alpha_2 r_s^{\gamma_2}$, and the parameters α_1, α_2 and γ_1, γ_2 can be found in Ref. [35].

Now we consider the exact solution of the dispersion equation $\varepsilon(z,u)=0$ for an interacting electron gas when the DF is given by LFC expression (13). From Eqs. (6)–(8), (13), and (14), it is seen that the collective plasma modes (plasmons) can propagate with the frequency and momentum ω and k (or u and z) which lie in the domain $u\geq z+1$ where $f_2(z,u)=0$ and $\mathrm{Im}[\varepsilon(z,u)]=0$. In this domain, the dispersion equation has an exact analytical solution which, in Lindhard's dimensionless variables, is given by

$$u_r^2(z) = 1 + z^2[\alpha z g(z) + 1]^2 + \frac{1}{\alpha z g(z)[\alpha z g(z) + 2]}, \tag{16}$$

with $\alpha=\sqrt{2}/r_s$ and $g(z)=[1-G(z)]^{-1}$. It is straightforward to check that the solution (16) indeed satisfies the condition $u_r(z)\geq z+1$ for arbitrary z. However, an inspection of the dispersion equation shows that this solution exists only for the wave numbers from the domain $0\leq k\leq k_c$ (or $0\leq z\leq z_c$) where the critical wave number z_c is obtained from an equation $u_r(z_c)=1+z_c$, i.e., in this point, the plasmon curve $u_r(z)$ touches to the boundary of the single-particle continuum $u=1+z$. Explicitly, the critical wave numbers are determined from transcendental equation

$$\alpha z_c^2 g(z_c)[2 + \alpha z_c g(z_c)] = 1. \tag{17}$$

Table I shows the quantity z_c and the minimum of the dispersion function $\lambda_c=u_r(z_{\min})$ with $u_r'(z_{\min})=0$ for some values of the density parameter r_s. The critical wave numbers and the quantities λ_c (labeled as $z_c^{(0)}$ and $\lambda_c^{(0)}$, respectively) are also shown for noninteracting electron gas, i.e., with $G(z)=0$ and $g(z)=1$. These quantities are important for evaluation of the SP in Sec. III.

We can present the dispersion expression (16) obtained above, in the usual form

$$\omega_r^2(k) = \omega_p^2(k)\frac{2/g(k) + k\lambda_{\mathrm{TF}}g(k)}{2 + k\lambda_{\mathrm{TF}}g(k)} + k^2v_F^2\frac{2 - \frac{1}{2}g(k) + k\lambda_{\mathrm{TF}}g(k)}{2 + k\lambda_{\mathrm{TF}}g(k)} + \frac{\hbar^2k^4}{4m^2}[1 + k\lambda_{\mathrm{TF}}g(k)]^2, \tag{18}$$

which for vanishing exchange-correlation interactions [i.e., at $g(k)=1$] reads

$$\omega_r^2(k) = \omega_p^2(k) + k^2v_F^2\frac{3 + 2k\lambda_{\mathrm{TF}}}{4 + 2k\lambda_{\mathrm{TF}}} + \frac{\hbar^2k^4}{4m^2}(1 + k\lambda_{\mathrm{TF}})^2. \tag{19}$$

This exact (within the employed model) dispersion relation may be compared to an approximate result derived by Fetter within a hydrodynamical approach [36]. Equation (19) agrees with the hydrodynamic result if the last term (the single-particle energy) in this expression is neglected and the coefficient at $k^2v_F^2$ is replaced by a constant factor 1/2. It

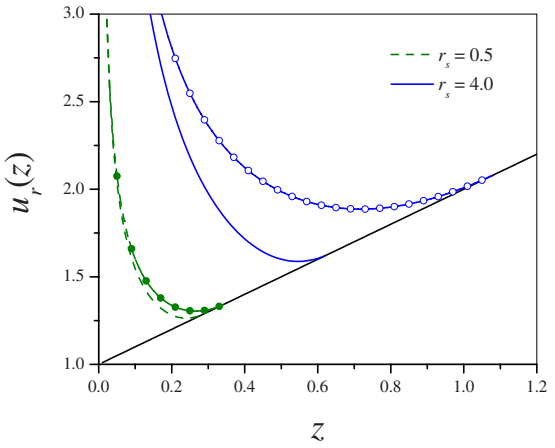

FIG. 3. (Color online) The dispersion curve $u_r(z)$ for free (lines with symbols) and interacting (lines without symbols) electron gases vs z for r_s=0.5 (dashed lines) and r_s=4.0 (solid lines). Oblique solid line corresponds to $\omega = kv_F + \hbar k^2/2m$ (or $u = z+1$).

should be emphasized that in general and at long wavelengths $\omega_r(k)$ from Eq. (18) for an interacting 2D electron system varies like $k^{1/2}$ independently of the static LFC $G(k)$ and in contrast to the 3D case. This latter behavior seems first to have been suggested by Ferrell [37] and later investigated in more detail by Stern [31] (see also the review paper [33]). It arises from the electromagnetic fields in the vacuum surrounding the plane, with an associated reduction in the screening. Since $\omega_r(k)$ increases monotonically from zero, an external perturbation of arbitrarily low frequency can always excite collective modes. Hence, the characteristic 3D absorption edge at constant 3D ω_p is here entirely absent. Moreover, the group and phase velocities both diverge like $k^{-1/2}$ as $k \to 0$.

Figure 3 shows the plasmon dispersion curve $u_r(z)$ for interacting (the lines without symbols) and noninteracting (the lines with symbols) electron gases, i.e., Eqs. (16) and (19), respectively. The points where the plasmon curves touch the single-particle excitation boundary are given by z_c or $z_c^{(0)}$ (see Table I). It is seen that the exchange-correlation interaction may strongly reduce the values of $u_r(z)$. It must be pointed out a technical but important detail which, to our knowledge, has not been yet discussed in the literature. From Fig. 3, it is seen that in u,z plane, the plasmon curve $u_r(z)$ has a minimum which is absent in usual units ω,k, where $\omega_r(k)$ is a monotonic increasing function. By interchanging the z and u axes in Fig. 3, one obtains the plasmon dispersion curve $z_r(u)$ which, however, in contrast to the 3D case has two different branches with increasing $[z_{r1}(u)]$ and decreasing $[z_{r2}(u)]$ dispersion functions [at the minimum of $u_r(z)$, both $z_{r1}(u)$ and $z_{r2}(u)$ curves contact each other]. The dispersion relations $z_{r1}(u)$ and $z_{r2}(u)$ can be provisionally treated as the "single-particle" and "plasmonic" relations, respectively. Therefore, when one attempts to perform z integration in the SP formula [see Eq. (20) below] before u integration, as was done in Ref. [6], the double integration in the SP is reduced to two line integrations along the contours $z_{r1}(u)$ and $z_{r2}(u)$ and both of them contribute to the SP. In other words, in this case, the energy loss function $L(z,u)$ introduced above contains two Dirac δ functions. In fact, we see from our numerical calculations that near the SP maximum, the contribution of $z_{r1}(u)$ is not necessarily small compared to the contribution of the other one, $z_{r2}(u)$, although the total contributions of both in the SP are in general much smaller than the purely single-particle contributions. This is a violation of the Lindhard-Winther equipartition sum rule [18] which we further discuss in Sec. III A. To avoid this technical problem in the numerical calculations, it is easier to perform first in Eq. (20) the u integration and then using the dispersion function $u_r(z)$ given by Eq. (16).

III. STOPPING POWER

With the theoretical formalism presented so far, we now take up the main topic of this paper. This is to study the SP of a pointlike ion in a 2D degenerate electron gas as well as to show how collective and single-particle excitations in the target medium contribute to the SP. Moreover, as in the previous section, we shall present theoretical results within the linear-response approach. We consider two models for a DEG in 2D. (i) A damping-inclusive DEG for which we use a number-conserving DF given in Eqs. (1)–(5). For this case, we present analytical calculations and results for the SP in a low-velocity limit. (ii) A strongly coupled DEG with a DF which includes static LFC, Eqs. (13) and (14). This case has been studied in Refs. [6,7] where the leading term in a high-velocity limit of the SP is calculated using a plasmon-pole approximation. This calculation is supported by a more rigorous treatment, again for the leading term only, in Refs. [8,9] which is based on a method of moments and includes electron-electron interactions. Now the leading term happens not to depend on electron-electron interaction. It is then of interest to calculate analytically the next nonvanishing terms of the high-velocity SP. As shown below, these terms are significantly modified by electron-electron interaction and thus are more involved than the leading term.

We consider an external point-like projectile of charge Ze moving with velocity $\mathbf{v}$ in a homogeneous and isotropic 2D electron medium characterized by the dielectric function $\varepsilon(k,\omega)$ or $\varepsilon(z,u)$. Then in the linear-response theory, the SP which is the energy loss per unit length by this projectile is given by [3,6]

$$S = \frac{8\Sigma_0 Z^2}{\pi \chi^4 \lambda} \int_0^{\lambda} \frac{u du}{\sqrt{\lambda^2 - u^2}} \int_0^{\infty} \mathrm{Im} \frac{-1}{\varepsilon(z,u)} z dz. \tag{20}$$

Here, $\lambda = v/v_F$ and $\Sigma_0 = e^2/a_0^2$. We have used the Lindhard variables z and u introduced in Sec. II. In our calculations, we shall consider the range of v for which the linear-response theory is found to be adequate [38].

A. Equipartition sum rule

With the theoretical formalism presented so far, we now take up one of the main topics of this paper. This is to study how collective and single-particle excitations in the 2D electron gas contribute to the SP. This problem was first addressed by Lindhard and Winther [18] (LW) for a 3D degenerate electron gas without damping (γ=0). They formulated

an equipartition sum rule which states that an integral proportional to that in Eq. (20)

$$\mathcal{I}(u) = \mathcal{I}_{sp}(u) + \mathcal{I}_p(u) = \int_0^\infty \mathrm{Im}\frac{-1}{\varepsilon(z,u)} z dz \tag{21}$$

receives equal contributions from plasmon ($\mathcal{I}_p$) (with $0<z<u-1$) and from single-particle excitations ($\mathcal{I}_{sp}$) (with $u-1<z<u+1$), respectively. The functions $\mathcal{I}_p(u)$ and $\mathcal{I}_{sp}(u)$ may then be written as

$$\mathcal{I}_p(u) = \int_0^{u-1} \mathrm{Im}\frac{-1}{\varepsilon(z,u)} z dz = \frac{\pi z_r(u)}{\left|\frac{\partial}{\partial z}\varepsilon(z,u)\right|_{z=z_r(u)}}, \tag{22}$$

$$\mathcal{I}_{sp}(u) = \int_{u-1}^{u+1} \mathrm{Im}\frac{-1}{\varepsilon(z,u)} z dz. \tag{23}$$

Here, $z_r(u)$ is the solution of the dispersion equation $\varepsilon(z,u)=0$ [the inverse of the dispersion function $u_r(z)$]. This equipartition rule is valid for sufficiently large u, $u>u_m$, where the threshold value u_m in 3D case is obtained from the equation $z_r(u_m)=u_m-1$. In recent works [21,24,39], we have shown that the LW equipartition rule does not necessarily hold for an extended charged projectile, e.g., a diproton cluster in a 3D degenerate electron gas without damping ($\gamma=0$) as well as for a pointlike ion in a damping-inclusive DEG. We have established some generalized stopping-power sum rules. In this section, we briefly show that the LW equipartition rule is also violated for a 2D electron gas. In the present context, it should be emphasized that the plasmon contribution given by Eq. (22) contains indeed two terms, with $z_{r1}(u)$ and $z_{r2}(u)$, as discussed above. The existence of both branches requires the threshold condition $u>u_m$, where u_m is the minimum value of the dispersion function $u_r(z)$ shown, e.g., in Fig. 3. However, it is clear that the contribution of $z_{r1}(u)$ vanishes at $u>u_c$, where $u_c=u_r(z_c)>u_m$ (the point where the plasmon curve touches to the single-particle excitations boundary). For simplicity, we consider below only the domain $u>u_c$, where only $z_{r2}(u)\equiv z_r(u)$ contributes to the SP integral (22). As an example, we employ the DF (13) together with Eqs. (6)–(8) and (14) for an interacting DEG. The simplest way to show the violation of the LW equipartition rule in 2D is to calculate the asymptotic values of the contributions $\mathcal{I}_p(u)$ and $\mathcal{I}_{sp}(u)$ at $u\gg 1$. The inverse dispersion function $z_r(u)$ for 2D interacting DEG is evaluated in Appendix B [see Eqs. (B5) and (B6)]. Using these expressions, it is straightforward to calculate the single-particle and collective contributions to the SP integral which at $u\gg 1$ become

$$\mathcal{I}_p(u) \simeq \frac{\pi}{4\alpha^2 u^4}\left\{1 + \frac{3-2\varkappa(r_s)}{2u^2} + \frac{3}{4u^4}\left[\varkappa^2(r_s) - 3\varkappa(r_s) + \frac{29}{12}\right] + \cdots\right\}, \tag{24}$$

$$\mathcal{I}_{sp}(u) \simeq \frac{\pi}{4\alpha u}\left\{1 + \frac{1}{4u^2} + \frac{1}{2\alpha u^3}\left[1 - \frac{\varkappa(r_s)}{\varkappa_0(r_s)}\right] + \frac{1}{8u^4} + \cdots\right\}. \tag{25}$$

Here, $\varkappa_0(r_s)$ and $\varkappa(r_s)$ are defined in Appendix B. From the above expressions, it is clear that the contribution of the collective excitations is much smaller than the contribution from single-particle excitations, $\mathcal{I}_p(u)\ll\mathcal{I}_{sp}(u)$, which indicates the violation of the LW equipartition rule. A similar result has been found numerically in Ref. [6] and is supported by our own numerical calculations. Of course, Eqs. (24) and (25) are not strong results. An exact treatment can be developed on the basis of the integration contour on the complex z plane suggested by LW [18] and investigated in details in Ref. [24]. The technique developed in [24] is independent of the dimensionality of electron gas but requires a necessary analytic continuation of the DF in the complex z plane, that is $\varepsilon(-z^*,u)=\varepsilon^*(z,u)$, where the asterisk indicates a complex-conjugate quantity. It is easy to see that this condition is violated for a 2D electron gas. For simplicity, let us consider noninteracting DEG with the DF given by Eq. (2) in the integral form and with $\Gamma\to+0$. In this case, one can easily check that $\varepsilon_{\mathrm{RPA}}(-z^*,u)=2-\varepsilon^*_{\mathrm{RPA}}(z,u)$ (a similar equation can be obtained for an interacting electron gas). Therefore an arbitrary function of the form

$$\varepsilon_{\mathrm{eff}}(z,u) = 1 + \frac{\mathcal{C}}{z}[\varepsilon_{\mathrm{RPA}}(z,u) - 1], \tag{26}$$

with an arbitrary constant $\mathcal{C}$ defines an effective DF of a 2D electron gas which satisfies the required condition, i.e., $\varepsilon_{\mathrm{eff}}(-z^*,u)=\varepsilon^*_{\mathrm{eff}}(z,u)$. Applying now the contour integration technique developed in Ref. [24], one can strongly prove that the single-particle and collective excitations contribute equally to the SP integral (21) where the DF $\varepsilon(z,u)$ is replaced by the effective one, $\varepsilon_{\mathrm{eff}}(z,u)$, given by Eq. (26). Thus the LW equipartition rule holds also in 2D treating the effective DF instead of $\varepsilon(z,u)$. In this case, it is straightforward to check that at $u\gg 1$, the leading-order terms of the collective and single-particle excitations are given by $\mathcal{I}_p(u)=\mathcal{I}_{sp}(u)\simeq\pi/(4\alpha u^2)$. The physical origin of the modification of the equipartition rule in 2D is the change of the nature of the Coulomb potential (in Fourier space, it behaves as $\sim 1/k$ in 2D) and as a consequence, the long-wavelength dispersion relation: the plasma frequency behaves as $\sim k^{1/2}$ in this limit. Technically, this modification introduces an extra noncompensated z variable as a prefactor in Eq. (2), first line, which changes the analytical properties of the DF. Introducing an effective DF (26), we formally replace the 2D Coulomb potential by the 3D one without affecting the polarizability of the 2D system. This recovers formally the 3D-type dispersion relation with constant plasma frequency and hence the equipartition rule.

B. Low-velocity limit

Let us consider SP for slow projectiles, with $v\ll v_F$. A consequence of the 3D linear-response theory, confirmed by experiments, is that for ion velocities v low compared to the Fermi velocity v_F, the stopping power is proportional to v

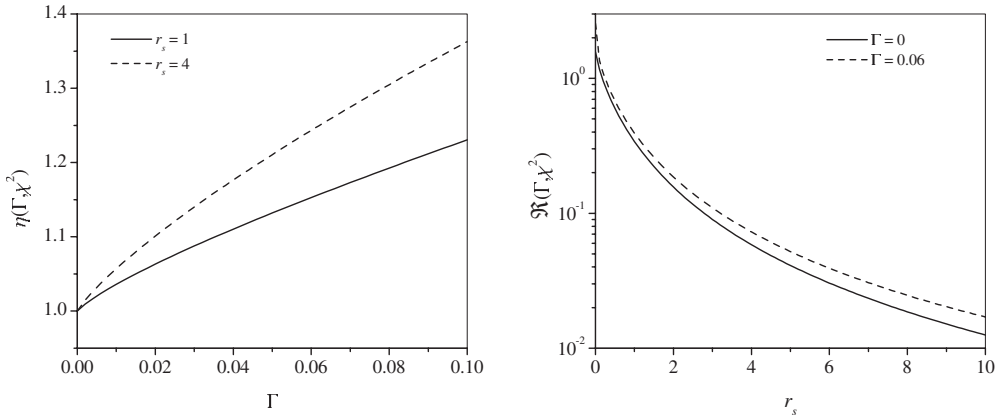

FIG. 4. (Left panel) The ratio of the friction coefficients with and without damping $\eta(\Gamma,\chi^2)=\Re(\Gamma,\chi^2)/\Re_0(\chi^2)$ vs dimensionless damping parameter Γ for various densities. $r_s=1$ (solid line), $r_s=4$ (dashed line). (Right panel) The friction coefficient $\Re(\Gamma,\chi^2)$ vs density parameter r_s for $\Gamma=0$ (solid line) and $\Gamma=0.06$ (dashed line).

(see, e.g., the latest experiment [40]). The coefficient of proportionality may be called a friction coefficient. A similar linear behavior of the SP, $S\sim v$, is expected in 2D case Refs. [3–7]. Using analytical results obtained for $\varepsilon_{\mathrm{RPA}}(z,u,\Gamma)$, the general expression for SP follows from Eq. (20) with Eqs. (1)–(5):

$$S \simeq \frac{2\Sigma_0 Z^2}{\chi^2}\lambda\int_0^\infty \frac{\Xi(z,\Gamma)z^4dz}{[z^2+\chi^2 f(z)]^2} = \frac{2\Sigma_0 Z^2}{\chi^2}\lambda\Re(\Gamma,\chi^2), \tag{27}$$

where the dimensionless friction coefficient $\Re(\Gamma,\chi^2)$ depends on the target properties and hence also on the dimensionless damping parameter Γ. We have introduced the following functions:

$$\Xi(z,\Gamma) = \frac{1}{\Gamma}\frac{f(z)[2f(z)-\psi(z,\Gamma)]}{\psi(z,\Gamma)}, \tag{28}$$

$$\psi(z,\Gamma) = F_1(z,0,\Gamma) = 2z + \frac{\Gamma}{z}[\Phi_-(z)-\Phi_-(-z)] - (z+1)\Phi_+(z) - (z-1)\Phi_+(-z), \tag{29}$$

$$\Phi_\pm(z) = \frac{1}{\sqrt{2}}\sqrt{\sqrt{\frac{z^2(z-1)^2+\Gamma^2}{z^2(z+1)^2+\Gamma^2}} \pm \frac{z^2(z^2-1)+\Gamma^2}{z^2(z+1)^2+\Gamma^2}}. \tag{30}$$

The static screening function $f(z)$ is determined from Eq. (10).

When the damping vanishes ($\Gamma\to 0$), Eq. (29) becomes

$$\psi(z,\Gamma) \to 2f(z) - \frac{2\Gamma}{\sqrt{1-z^2}}H(1-z) + \mathrm{O}(\Gamma^2), \tag{31}$$

where $H(z)$ is the Heaviside unit-step function. Therefore,

$$\Xi(z,\Gamma\to 0) = \frac{1}{\sqrt{1-z^2}}H(1-z) \tag{32}$$

and from Eq. (27) we find

$$\Re(\Gamma\to 0,\chi^2) = \Re_0(\chi^2) = \int_0^1 \frac{z^2dz}{(z+\chi^2)^2\sqrt{1-z^2}} = \frac{\pi}{2} + \frac{\chi^2}{1-\chi^4}\left[1 + \frac{2(\chi^4-2)}{\sqrt{|\chi^4-1|}}\mathcal{G}(\chi^2)\right], \tag{33}$$

with

$$\mathcal{G}(x) = \begin{cases} \arctan\sqrt{\dfrac{x-1}{x+1}}, & x>1 \\ \dfrac{1}{2}\ln\left(\dfrac{1}{x}+\sqrt{\dfrac{1}{x^2}-1}\right), & x<1. \end{cases} \tag{34}$$

The last expressions (33) and (34) are known results derived previously within RPA in Refs. [3,6]. Interestingly, in a low-velocity limit, this SP completely agrees with the result obtained within a binary collision approach [10]. In left panel of Fig. 4, we show the ratio of the damping-inclusive friction coefficient $\Re(\Gamma,\chi^2)$ and $\Re_0(\chi^2)$ vs damping parameter Γ for two values of the density parameter $r_s=1$ and $r_s=4$. To gain more insight in right panel of Fig. 4, we show the friction coefficient $\Re(\Gamma,\chi^2)$ vs r_s for two values of the damping parameter Γ. As expected, the friction coefficient and hence the SP at low velocities increase with an increasing damping parameter γ; this was previously reported for 3D in Refs. [23–25]. We will further discuss this behavior in Sec. IV.

The approximation (27) implies that the SP is proportional to velocity. The velocity region in which the linear proportionality between SP and the projectile velocity holds may be inferred from the numerical examples given in Sec. IV. It is seen from those results that the approximation (27) remains quite accurate even when λ becomes as large as ~ 1.

C. High-velocity limit

Consider next the limit of large projectile velocities in the case of strongly interacting DEG with the dielectric function Eqs. (13)–(15). In this limit, the general expression (20) for pointlike projectiles with charge Ze moving in either interacting or free-electron gas reduces to the simple formula [3]

$$S \simeq \frac{\pi\Sigma_0 Z^2}{\chi^2\lambda} = \frac{2\pi^2 n_0 Z^2 e^4}{\hbar v}, \tag{35}$$

which does not contain the electron mass m anymore; m and also the effects of electron-electron interactions appear only in the higher terms of the expansion. The other main discrepancy between the 2D and the 3D results is that the stopping power decreases as $1/v$ instead of behaving as $\ln v/v^2$ in the 3D case. In the presence of interactions, the next-order terms are shown to be significantly modified. We derive below a generalized expression for SP, in a high-velocity limit, for pointlike ions. In order to show how SP in a high-velocity limit is affected, we consider expression (20) rewritten as follows:

$$S = \frac{2\Sigma_0 Z^2}{\chi^2\lambda}\int_0^\lambda \frac{\Lambda(u)du}{\sqrt{\lambda^2-u^2}}, \tag{36}$$

where

$$\Lambda(u) = \frac{4\alpha}{\pi}u\mathfrak{I}(u) = \frac{4\alpha}{\pi}u\int_0^\infty \mathrm{Im}\frac{-1}{\varepsilon(z,u)}zdz \tag{37}$$

and $\mathfrak{I}(u)$ is the total contribution of the collective and single-particle excitations to the SP integral defined in Sec. III A [see Eqs. (21)–(23)]. For further progress, it is imperative to calculate the asymptotic behavior of the function $\Lambda(u)$ at $u\to\infty$. For collective and single-particle excitations, these asymptotic forms are given by Eqs. (24) and (25), respectively. Using these expressions, we arrive at

$$\Lambda(u) = 1 + \frac{C_2}{u^2} + \frac{C_3}{u^3} + \mathrm{O}(u^{-4}) \tag{38}$$

for $u\to\infty$ and with the expansion coefficients

$$C_2 = \frac{1}{4}, \quad C_3 = \frac{3}{2\alpha}[1-\varkappa_1(r_s)]. \tag{39}$$

Here, the parameter $\varkappa_1(r_s)$ depends on the exchange-correlation interactions and is given explicitly in Appendix B.

Below, we calculate the SP up to the order $\mathrm{O}(v^{-4})$ thus neglecting the terms with $\mathrm{O}(\lambda^{-5})$. First, the SP (36) can be represented in the equivalent form

$$S = \frac{\pi\Sigma_0 Z^2}{\chi^2\lambda}\left\{1 + \frac{h_1}{\lambda} + \frac{1}{2\pi\lambda^2}\left[1 - \frac{1}{\lambda+\sqrt{\lambda^2-1}} - \Phi_2(\lambda)\right] + \frac{C_3}{\pi\lambda^3}\left[\frac{3}{2} + \frac{1}{4C_3} - \frac{\lambda}{\lambda+\sqrt{\lambda^2-1}} + \ln(\lambda+\sqrt{\lambda^2-1}) + \Phi_1(\lambda)\right]\right\}, \tag{40}$$

which is convenient for further calculations. Here h_1 is a constant

$$h_1 = \frac{2}{\pi}\int_0^\infty [\Lambda(u)-1]du \tag{41}$$

and the other quantities are function of the ion velocity

$$\Phi_1(\lambda) = \frac{2\lambda^2}{C_3}\int_0^1 \left(\frac{1}{\sqrt{1-u^2/\lambda^2}} - 1\right)[\Lambda(u)-1]du + \frac{2\lambda^2}{C_3}\int_1^\lambda \left(\frac{1}{\sqrt{1-u^2/\lambda^2}} - 1\right) \times \left[\Lambda(u) - 1 - \frac{C_2}{u^2} - \frac{C_3}{u^3}\right]du - \frac{1}{2} - \frac{1}{4C_3}, \tag{42}$$

$$\Phi_2(\lambda) = 4\lambda\int_\lambda^\infty [\Lambda(u)-1]du. \tag{43}$$

For the derivation of Eq. (40), we have used some elementary integrals [34]. In Appendix B, we prove that $h_1=0$ [see Eq. (B8)]. This relation can be regarded as another SP sum rule for an interacting DEG.

For a calculation of the SP up to fourth order v^{-4}, we need the asymptotic behavior of $\Phi_2(\lambda)$ up to the first order (v^{-1}) which can be obtained from Eqs. (38) and (43),

$$\Phi_2(\lambda) = 1 + \frac{2C_3}{\lambda} + \mathrm{O}(\lambda^{-2}), \tag{44}$$

and only the leading term of $\Phi_1(\lambda)$. We denote this leading term by $\Phi_1(\lambda\to\infty)=\ln h_2$ and using Eq. (42), we obtain

$$\ln h_2 = \frac{1}{C_3}\left\{\int_0^1 [\Lambda(u)-1]u^2du + \int_1^\infty \left[\Lambda(u) - 1 - \frac{C_2}{u^2} - \frac{C_3}{u^3}\right]u^2du - \frac{1}{4}\right\} - \frac{1}{2}. \tag{45}$$

The coefficient $\ln h_2$ is explicitly evaluated in Appendix B and entirely depends on the density parameter r_s [see Eq. (B14)]. Thus, substituting Eqs. (44) and (45) into Eq. (40) and setting $h_1=0$, we finally obtain

$$S \simeq \frac{\pi\Sigma_0 Z^2}{\chi^2\lambda}\left[1 + \frac{C_3}{\pi\lambda^3}\ln(2h_2\lambda)\right]. \tag{46}$$

It is seen that in the correction term [the second term in Eq. (46)], the mass of electron enters through the Fermi velocity $v_F=\hbar k_F/m$. A limit to the noninteracting DEG is performed by taking the limit $\varkappa_1(r_s)\to 0$, i.e., setting $C_3=3/2\alpha = (3\sqrt{2}/4)r_s$ [see Eq. (39)]. In this limit, the coefficient $\ln h_2$ is given by Eq. (B15). In the general case of nonvanishing exchange-correlation interactions, it is too difficult to draw some conclusions from Eq. (46) about how these interactions affect the high-velocity SP. Numerical calculations of Refs. [6,7] show that these interactions strongly increase the SP up to the intermediate velocity range with $v\sim v_F$. We support this conclusion by our own calculations (not shown here) which also indicate that the asymptotic SP (46) remains quite accurate also in the intermediate velocity range.

We close this section with the following two remarks. First, the high-velocity SP Eq. (46) is also valid for a general LFC function $G(k)$. The derivations above and in Appendix B show that only the asymptotic values of $G(k)$ at $k\to\infty$ and $k\to 0$ contribute to Eq. (46). At short wavelengths,

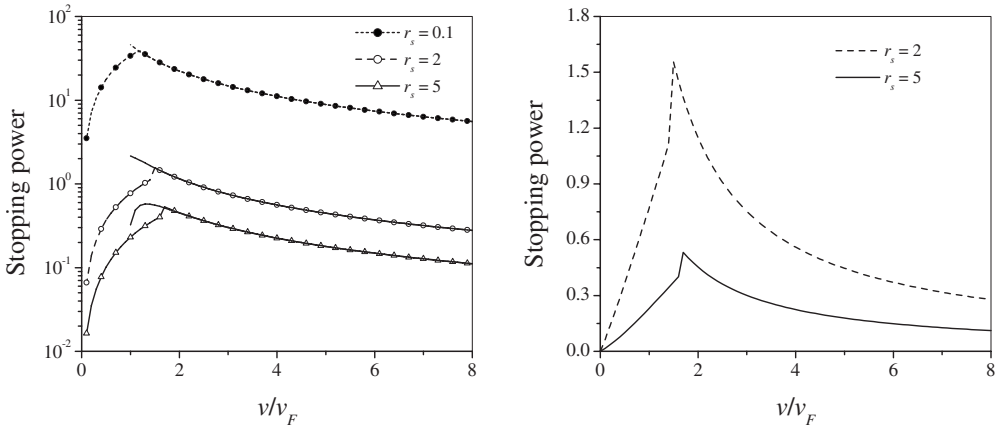

FIG. 5. (Left panel) The SP (in units of Σ_0 and in logarithmical scale) of a proton vs v/v_F moving in an interacting electron gas for $r_s=0.1$ (dotted line), $r_s=2$ (dashed line), and $r_s=5$ (solid line). The lines with and without symbols correspond to the numerical evaluation of Eq. (20) with Eqs. (13)–(15) and asymptotic expression (46), respectively. (Right panel) Dashed and solid lines (with symbols) from the left panel in linear scale.

$G(k\to\infty)=G_\infty(r_s)$ is constant (see, e.g., Ref. [35]). At long wavelengths, the static LFC function behaves as $G(k\to 0)\simeq\kappa(r_s)k/k_F$, where the constant $\kappa(r_s)$ is related to the compressibility of a 2D electron gas through compressibility sum rule. The latter for a 3D electron gas is discussed in [41] and for a 2D electron gas in [42]. Thus, in the general case of arbitrary $G(k)$, the quantities $\varkappa_1(r_s)$ and $\varkappa_2(r_s)$ in Eq. (46) are replaced by $\varkappa_1(r_s)=(1/3)G_\infty(r_s)$ and $\varkappa_2(r_s)=G_\infty(r_s)/4\kappa(r_s)$, respectively. Second, a similar procedure is applicable to evaluate the high-velocity corrections also for a damping-inclusive 2D electron gas. While the high-velocity SP (46) does not contain the terms of the second v^{-2} and third v^{-3} orders, some preliminary investigations by us show that for a damping-inclusive DEG, this SP involves also the terms of the order B_1v^{-2}, $B_2v^{-2}\ln v$, and $B_3v^{-2}\ln^2 v$, where the constants B_1, B_2, and B_3 depend on γ. Therefore, the corrections to the high-velocity SP would be much more sensitive to the ion velocity than those predicted by Eq. (46).

IV. NUMERICAL EXAMPLES

Using the theoretical results obtained in Secs. II and III, we present here the results of our numerical calculations of stopping power for a 2D target material with the wide range of the density parameter, $0.1\le r_s\le 5$. The parameter r_s varies from the small (free DEG) up to the large (strongly interacting DEG) values. As examples of 2D target material, we have considered two models. An interacting DEG whose linear-response function includes the exchange-correlation effects via static LFC and is given by Eqs. (13)–(15). This case has been investigated previously in Refs. [6,7]. In Fig. 5 left panel, we compare the exact (the lines with symbols) and asymptotic (the lines without symbols) SPs calculated from Eqs. (20), (13)–(15), and (46), respectively. It is seen that the asymptotic expression (46) is very accurate and at $v\gtrsim v_F$ practically coincides with exact SP. In general, we have found that the higher-order correction in Eq. (46) (the second term) is small compared to the leading term. However, the role of this term becomes more and more pronounced with increasing the density parameter r_s, i.e., with increasing the exchange-correlation interactions. We have also compared our numerical calculations to the results obtained by Wang and Ma [6,7]. Two major differences have been found. First, the LFC dielectric function (13) for a fully degenerate electron gas predicts a threshold ion velocity for plasmon excitations. In view of the discussion in Sec. II B, the plasmons are excited at $\lambda>\lambda_c$, where the critical (dimensionless) velocity λ_c is the minimum value of the dispersion function $u_r(z)$, Eq. (16), and can be found from the equations $\lambda_c=u_r(z_{\min})$ with $u_r'(z_{\min})=0$ (see also Table I). The velocity threshold changes sufficiently the slope of the SP and at $\lambda=\lambda_c$ one expects a characteristic discontinuity of the derivative of the SP (the SP itself remains naturally continuous at $\lambda=\lambda_c$). In contrast to Refs. [6,7], this feature is clearly visible in Fig. 5, right panel (see also the solid lines in Fig. 6). Such behavior of the SP at $\lambda=\lambda_c$ has been observed previously in 3D (see, e.g., [43] and references therein).

Second, we have found that for the same conditions (i.e., for the same r_s), the SP in our case is considerably smaller near maximum than those obtained in Ref. [6]. Moreover, there is no agreement between the results obtained in Refs. [6,7], e.g., for $r_s=1$ and $r_s=5$, where Ref. [6] predicts in whole velocity range much larger SP than the latter. Apparently this is because the polarizability of the free-electron gas employed in Ref. [6] somewhat differs from original expression derived by Stern [31] [see also Eq. (14) with Eqs. (6) and (7)]; the algebraic square roots in Eqs. (6) and (7) are missing in Ref. [6]. These square roots are recovered in Ref. [7] but nevertheless one of two plasmon branches is ignored as discussed in Sec. II B which may yield smaller value of the SP.

Within the second model, the target material is modeled as an electron gas whose linear-response function, within RTA, is given by Eqs. (1)–(5) with γ as a model damping parameter. In Fig. 6, we compare the SP obtained for a damping-inclusive 2D DEG [with $\Gamma=0.06$ (dashed lines) and $\Gamma=0.1$ (dotted lines)] with those for a vanishing damping (solid lines). It is seen from Fig. 6 that the SP is broadened with increasing damping parameter γ. Of course, the value

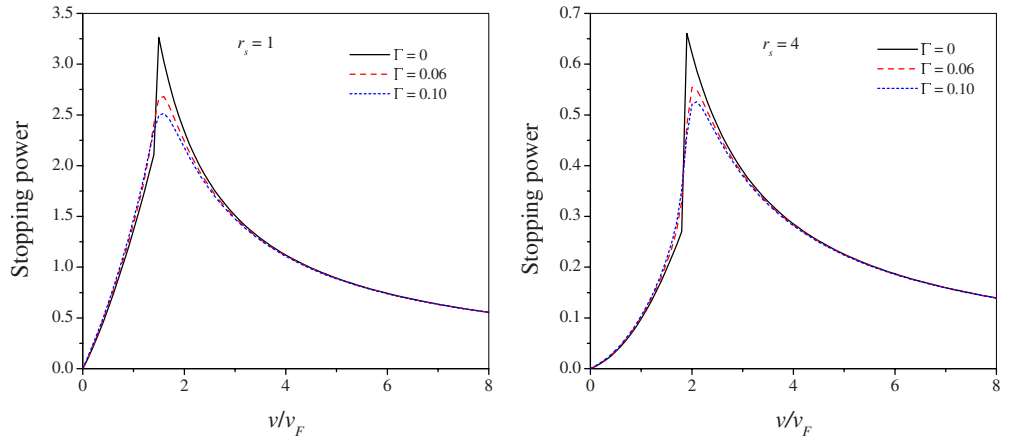

FIG. 6. (Color online) The SP (in units of Σ_0) of a proton vs v/v_F moving in a damping-inclusive electron gas for $\Gamma=0$ (solid line), $\Gamma=0.06$ (dashed line), $\Gamma=0.1$ (dotted line), $r_s=1$ (left panel), and $r_s=4$ (right panel).

$r_s=4$ in Fig. 6 (right panel) is somewhat far beyond the RPA employed for deriving the dielectric function Eqs. (1)–(5). However, treating this case as a qualitative example, we look for some complementary information about the effect of the damping at large r_s. In particular, at either vanishing or nonzero damping Fig. 6 (right panel) predicts a modification of the linear friction law [see Eq. (27)] which now approximately behaves as $\sim v^3$. This is v^3 law obtained, e.g., in Ref. [44] within linear-response theory for classical 3D plasma and supported by the numerical simulations [38]. According to Fig. 4 (right panel) the linear friction coefficient decays with r_s and may be smaller than the cubic friction coefficient ($\sim v^3$). It should be emphasized, however, that in the present context of a DEG the friction is closely related to the Pauli constraint which restricts the dynamics of the electron-hole excitations and this restriction is expected to be more pronounced at small velocities.

V. SUMMARY AND CONCLUDING REMARKS

In this paper, we have presented a theoretical study of the stopping power of point-ion projectile in a degenerate 2D electron gas. The latter is modeled within two different approaches, namely, (i) as a system involving the collisions and (ii) including exchange-correlation interactions of the electrons. In the course of this study, we have also derived some analytical results for the damping-inclusive RPA linear-response function and for the corresponding plasmon dispersion relations. These analytical results go beyond those obtained previously in Refs. [28–30] within small-k,ω approximation. Also for the model (ii), we have found exact dispersion relations. After a general introduction to the SP of an ion in Sec. II, theoretical calculations of SP based on the linear-response theory and using the models (i) and (ii) are discussed in Sec. III. A number of limiting and asymptotic regimes of low and high velocities and vanishing damping have been studied. These approximate expressions are well supported by our numerical calculations. Special attention has been paid to the equipartition sum rule in 2D. In Sec. III, employing the model (ii), i.e., the static LFC dielectric function for an interacting DEG, we have shown that this rule does not necessarily hold in 2D and may be satisfied introducing an effective dielectric function (26). The theoretical expressions for a number of physical quantities derived in this paper lead to a detailed presentation, in Secs. II–IV, of a collection of data through figures on SP, friction coefficient, and the dispersion relations. For the dimensionless damping parameter, we have chosen the values $0<\Gamma\lesssim 0.1$; the damping parameters for some 2D metal and semiconductor materials fall within this range. The results we have presented demonstrate that with regard to several physical quantities of primary interest, the difference between RTA and usual RPA without damping is significant.

It is of particular interest to study the high-velocity limit for the SP of an ion beam. Such asymptotic expressions contain some useful information on a projectile ion structure factor and especially on the target medium properties. Equation (46) with Eq. (B14) which is a generalization of the asymptotic formula obtained in Refs. [3–6] can be used for analyses of experimental data on high-energy beam interactions with 2D target material. We note that the analytical method developed here for the derivation of high-velocity SP is general and may be applied within a linear-response treatment for other types of projectiles, e.g., extended multicharged ions, as well as for any particular form of the linear-response function $\varepsilon(z,u)$ for the target material. For given target material, this approach requires only the asymptotic form of the plasmon dispersion relation at high $u=\omega/kv_F$ and the frequency moments of the energy loss function. For a damping-inclusive DEG [model (i)], however, some modifications occur when one includes the damping in the DF. For instance, at large frequencies, the energy loss function $\mathrm{Im}[-1/\varepsilon(z,u)]$ for a DEG with collisions behaves as $\gamma\omega_p^2(k)/\omega^3$ and obviously the third frequency moment of this function does not exist [see Eq. (B9)]. This requires some additional investigation of the third moment sum rule for this case which in turn is important for evaluation of high-velocity SP (see Sec. III C).

We shall make some brief remarks on the RTA in the linear-response function. In the present study, the damping-inclusive linear-response function containing in the RTA has been considered only in RPA. Going beyond RPA with

electron-electron interaction and damping treated at the same microscopic level is a difficult task. We may mention that recently the linear-response function in 3D has been considered in RTA which conserves the particle number, momentum, and energy [45,46] (see also references therein). We intend to extend this model with fully conserving (number, momentum, and energy) linear-response function for 2D electron gas. The numerical values of the phenomenological quantity γ used in our calculations are within a physically expected range and can be estimated from the experimental data of the dc conductivity or the mobility in 2D systems [32,33].

An interesting issue not considered here is the dynamic LFC which may also lead to a damping of excitations because the imaginary part of $G(k,\omega)$ does not necessarily vanish. However, to our knowledge, the dynamic LFC to the DF has not been studied in detail for the 2D as for the 3D case. Since the dynamic LFC leads to a broadening of the energy loss function and a shortening of the excitations lifetime (compared to the static LFC), we expect qualitatively the same effect as in the damping-inclusive case; that is at low velocities, the SP increases and at intermediate velocities decreases with respect to the static LFC result (cf. Figs. 4 and 6).

We expect our theoretical findings to be useful in experimental investigations of ion-beam energy losses in solids. One of the improvements of our damping-inclusive model will be to include some short-range correlation in the linear-response function. We intend to take up further studies on interaction of charged projectiles with electron gas of lower dimensions.

ACKNOWLEDGMENTS

The work of H.B.N. has been partially supported by the Armenian Ministry of Higher Education and Science under Grant No. 87.

APPENDIX A: DIELECTRIC FUNCTION OF DAMPING-INCLUSIVE ELECTRON GAS

In this appendix, we give an alternative derivation of the damping-inclusive DF which is valid in the entire complex ω,k plane. Since we are going to compare our results to previous derivations in Refs. [28–30], here we use the usual energy (ω) and momentum (k) variables. Performing the q and θ integrations in Eq. (2) without splitting this expression into real and imaginary parts, for arbitrary ω and k complex variables, we obtain

$$\varepsilon_{\mathrm{RPA}}(k,\omega) = 1+\frac{2}{ka_0}\left[1-\frac{2\omega_+}{\sqrt{(\omega_+-\omega_k)^2-k^2v_F^2}+\sqrt{(\omega_++\omega_k)^2-k^2v_F^2}}\right], \tag{A1}$$

where $\omega_+=\omega+i\gamma$ and $\omega_k=\hbar k^2/2m$. Here $\hbar\omega_k$ is the single-particle energy and $\lambda_{\mathrm{TF}}=a_0/2$ plays a role of the Thomas-Fermi screening length which is constant in 2D case [36]. The multivalued functions in Eq. (A1) must be understood in the following way. (i) The imaginary parts of the square roots are positive. (ii) The signs of the real parts of the square roots with $\omega_+\pm\omega_k$ are taken with the sign of the expressions

$$\frac{|u_\pm|}{u_\pm}=\frac{|\omega\pm\hbar k^2/2m|}{\omega\pm\hbar k^2/2m}. \tag{A2}$$

These two conditions completely fix uniquely the values of the square roots entered in Eq. (A1). The full number-conserving DF is now evaluated using Mermin-Das formula, Eq. (1)

$$\varepsilon(k,\omega)=1+\frac{2}{ka_0}\left\{1-\frac{\omega+i\gamma Q(k,\omega)}{P(k,\omega)+i\gamma[Q(k,\omega)-1]}\right\}. \tag{A3}$$

Here,

$$P(k,\omega)=\frac{1}{2}[\sqrt{(\omega_+-\omega_k)^2-k^2v_F^2}+\sqrt{(\omega_++\omega_k)^2-k^2v_F^2}], \tag{A4}$$

$$Q(k,\omega)=\frac{2}{ka_0}\frac{1}{\omega_+}[P(k,\omega)-\omega_+]\left[\nu(k)-1-\frac{ka_0}{2}\right], \tag{A5}$$

$$\nu(k)=\frac{\varepsilon_{\mathrm{RPA}}(k,0)}{\varepsilon_{\mathrm{RPA}}(k,0)-1}=1+\frac{ka_0}{2}\frac{k/2k_F}{f(k/2k_F)}, \tag{A6}$$

and the function $f(z)$ has been introduced by Eq. (10).

Now let us consider the limit of small momentum-energy transfers, i.e., we assume that $k\ll 2k_F$ and $\hbar\omega\ll E_F$. In this case, $f(z)=z$ and the function Q in Eq. (A5) vanishes. In addition, neglecting the single-particle energies $\hbar\omega_k$ in Eqs. (A1), (A3), and (A4), we obtain

$$\varepsilon_{\mathrm{RPA}}(k,\omega)\simeq 1+\frac{2}{ka_0}\left(1-\frac{\omega_+}{\sqrt{\omega_+^2-k^2v_F^2}}\right) \tag{A7}$$

and

$$\varepsilon(k,\omega)\simeq 1+\frac{2}{ka_0}\left(1-\frac{\omega}{\sqrt{\omega_+^2-k^2v_F^2-i\gamma}}\right). \tag{A8}$$

These are precisely the same DFs obtained previously in Refs. [28–30] which used the same small k,ω approximation limits of the more general expressions (A1) and (A3). Note that the DFs (A7) and (A8) are the quasiclassical limits of the more general expressions (A1) and (A3), respectively. Therefore they can be alternatively derived from a classical kinetic equation within RTA with the Fermi distribution function as an unperturbed state.

APPENDIX B: EVALUATION OF THE PARAMETERS h_1 AND h_2

In this appendix, we give a detailed derivation of the parameters h_1 and h_2 which contributes to the high-velocity SP of an interacting 2D electron gas, Eqs. (41) and (45), respectively. First, we write Eq. (41) in another but equivalent form, $h_1=\wp(s\to\infty)$, where

$$\wp(s) = \frac{2}{\pi}\left[\int_0^s \Lambda(u)du - s\right] = \frac{8\alpha}{\pi^2}\left[\int_s^\infty zdz\int_0^s L(z,u)udu - \int_0^s zdz\int_s^\infty L(z,u)udu\right]. \tag{B1}$$

Here, $L(z,u)=\mathrm{Im}[-1/\varepsilon(z,u)]$ is the energy loss function. For the derivation of Eq. (B1), the Bethe sum rule (the first frequency moment of the energy loss function) in variables z and u has been used (see, e.g., Refs. [3,4,8])

$$\int_0^\infty \mathrm{Im}\frac{-1}{\varepsilon(z,u)}udu = \frac{\pi\chi^2}{4z} = \frac{\pi}{4\alpha z}. \tag{B2}$$

Assuming that the upper cutoff s is large enough, $s \gg 1$, Eq. (B1) can be written in explicit form

$$\wp(s) = \frac{8\alpha}{\pi^2}\left[\int_s^{s+1} zdz\int_{z-1}^s L(z,u)udu - \int_{s-1}^s zdz\int_s^{z+1} L(z,u)udu\right] - \frac{16\alpha^2}{\pi}\int_0^{z_r(s)} \frac{g(z)}{|g(z)|}\frac{z^3 g^2(z)u_r(z)dz}{|\phi_r(z)|}. \tag{B3}$$

Here, $u_r(z)$ is the solution of the dispersion equation for an interacting DEG, Eq. (16), and we have introduced a lower cutoff parameter $z_r(s)$ which $z_r(s)\to 0$ at $s\to\infty$. Also we have introduced the function $\phi_r(z)$ which is given by

$$\phi_r(z) = \frac{\partial}{\partial u}f_1(z,u)|_{u=u_r(z)} = \frac{u_r(z)-z}{\sqrt{[u_r(z)-z]^2-1}} - \frac{u_r(z)+z}{\sqrt{[u_r(z)+z]^2-1}}. \tag{B4}$$

The last term in Eq. (B3) is the contribution of the collective excitations and hence the function $f_1(z,u)$ in Eq. (B4) is defined in the domain $0<z<u-1$ (or $u>z+1$). Without loss of the generality, we chose as a lower cutoff [i.e., $z_r(s)$] a function which is inverse to $u_r(z)$. Using Eq. (16), it is straightforward to calculate the asymptotic behavior of this function at large u. It behaves as

$$z_r(u) = \frac{1}{2\alpha u^2}\left(1 + \frac{A_1}{u^2} + \frac{A_2}{u^4} + \frac{A_3}{u^6} + \cdots\right), \tag{B5}$$

where the expansion coefficients are given by

$$A_1 = \frac{3}{4} - \frac{1}{2}\varkappa(r_s),$$

$$A_2 = \frac{5}{8}[1-\varkappa(r_s)]\left[1-\frac{1}{2}\varkappa(r_s)\right] + \frac{\varkappa(r_s)}{16}[3-\varkappa(r_s)],$$

$$A_3 = \frac{35}{64} + \frac{1}{4\alpha^2} + \frac{\varkappa(r_s)}{16}\left[\varkappa_0^2(r_s) - 2\varkappa^2(r_s) + 9\varkappa(r_s) - \frac{29}{2}\right], \tag{B6}$$

with $\varkappa(r_s)=G_0(r_s)/[\alpha G_{12}(r_s)]$ and $\varkappa_0(r_s)=G_{22}(r_s)/[\alpha G_{12}(r_s)]$.

Since at small z the functions $u_r(z)$ and $\phi_r(z)$ behave as $u_r(z)\simeq(2\alpha z)^{-1/2}$ and

$$\phi_r(z) \simeq 4\alpha\sqrt{2\alpha}z^{5/2}\left\{1 + \frac{3\alpha z}{4}[1+2\varkappa(r_s)] + \mathrm{O}(z^2)\right\}, \tag{B7}$$

respectively, at $s\to\infty$ the plasmon contribution in Eq. (B3) vanishes as $\sim z_r(s)\sim s^{-2}\to 0$. For the calculation of the first two terms in Eq. (B3) (single-particle contributions), we first make a substitution of the integration variables, $z\to z+s$ and $u\to u+s$. At $s\to\infty$, the remaining expression behaves as $\wp(s)\simeq -1/(2\pi s)\to 0$. Thus at $s\to\infty$, $\wp(s)\to 0$ and

$$h_1 = \wp(s)|_{s\to\infty} = 0. \tag{B8}$$

For the calculation of the coefficient h_2, it is imperative to evaluate the third moment of the energy loss function. In 2D and in general case, this has been done in Ref. [8]. In the present context of an interacting electron gas with DF (13) and (14), this moment is given by

$$\int_0^\infty \mathrm{Im}\frac{-1}{\varepsilon(z,u)}u^3du = \frac{\pi}{8\alpha}\left\{\frac{1}{\alpha z^2}[1-G(z)] + \frac{3}{2z} + 2z\right\}. \tag{B9}$$

As we have done above, we represent now the coefficient h_2 through the relation $h_2=\mathfrak{I}(s\to\infty)$, where

$$\ln\mathfrak{I}(s) = \frac{1}{C_3}\int_0^s \Lambda(u)u^2du - \ln s - \frac{s}{4C_3} - \frac{s^3}{3C_3} - \frac{1}{2} \tag{B10}$$

and C_3 is given by Eq. (39). Employing the relation (B9) for the third frequency moment, we obtain

$$\ln\mathfrak{I}(s) = \frac{1}{3[1-\varkappa_1(r_s)]}[\ln(2\alpha) + 3\varkappa_1(r_s)\ln\varkappa_2(r_s)] - \frac{1}{2} - \frac{1}{2[1-\varkappa_1(r_s)]}U(s), \tag{B11}$$

where $\varkappa_1(r_s)=G_0(r_s)/[3G_{22}(r_s)]$ and $\varkappa_2(r_s)=G_{12}(r_s)/[2G_{22}(r_s)]$ are density-dependent parameters. The function $U(s)$ is evaluated in the similar way as we have done above. In particular, neglecting the contribution of plasmons which is again vanishingly small at $s\to\infty$, this function becomes

$$U(s) = \frac{16\alpha^2}{3\pi}\left[\int_{s-1}^s zdz\int_s^{z+1} L(z,u)u^3du - \int_s^{s+1} zdz\int_{z-1}^s L(z,u)u^3du - \frac{\pi s}{8\alpha}\right]. \tag{B12}$$

Now, only the single-particle excitation contributes to Eq. (B12). Again, by making the changes of the integration variables, $z \to z+s$ and $u \to u+s$, at $s \to \infty$, we have found that the function $U(s)$ behaves as

$$U(s) = \frac{1}{3} - \varkappa_1(r_s) + \frac{\alpha}{6s} + \mathrm{O}(s^{-2}). \tag{B13}$$

Finally, substituting Eq. (B13) into Eq. (B11) and taking the limit $s \to \infty$, we arrive at

$$\ln h_2(r_s) = \frac{1}{3[1-\varkappa_1(r_s)]}\left\{\ln\left(\frac{2\sqrt{2}}{r_s}\right) + 3\varkappa_1(r_s)[1+\ln \varkappa_2(r_s)] - 2\right\}. \tag{B14}$$

The transition to the limit of noninteracting 2D electron gas is performed by taking the limit $\varkappa_1 \to 0$ in Eq. (B14) which yields

$$\ln h_2(r_s) = \frac{1}{3}\left[\ln\left(\frac{2\sqrt{2}}{r_s}\right) - 2\right]. \tag{B15}$$

[1] A. C. Durst and S. M. Girvin, Science **304**, 1752 (2004).
[2] *Fundamental Phenomena in Low-Dimensional Electron Systems*, edited by M. Polini, M. Governale, V. Pellegrini, H. Grabert, and M. P. Tosi [Solid State Commun. **144** (2007), special issue].
[3] A. Bret and C. Deutsch, Phys. Rev. E **48**, 2994 (1993).
[4] A. Bret and C. Deutsch, Europhys. Lett. **25**, 291 (1994).
[5] A. Bret and C. Deutsch, Nucl. Instrum. Methods Phys. Res. A **415**, 703 (1998).
[6] Y. N. Wang and T. C. Ma, Phys. Lett. A **200**, 319 (1995).
[7] Y. N. Wang and T. C. Ma, Phys. Rev. B **52**, 16395 (1995).
[8] D. Ballester, A. M. Fuentes, and I. M. Tkachenko, Europhys. Lett. **75**, 791 (2006).
[9] D. Ballester, A. M. Fuentes, and I. M. Tkachenko, Phys. Rev. B **75**, 115109 (2007).
[10] I. Nagy, Phys. Rev. B **51**, 77 (1995).
[11] A. Krakovsky and J. K. Percus, Phys. Rev. B **52**, R2305 (1995).
[12] A. Bergara, I. Nagy, and P. M. Echenique, Phys. Rev. B **55**, 12864 (1997).
[13] Y. N. Wang and T. C. Ma, Phys. Rev. A **55**, 2087 (1997).
[14] A. Bergara, J. M. Pitarke, and P. M. Echenique, Phys. Rev. B **59**, 10145 (1999).
[15] E. Zaremba, I. Nagy, and P. M. Echenique, Phys. Rev. B **71**, 125323 (2005).
[16] H. A. Bethe, Ann. Phys. **397**, 325 (1930); F. Bloch, *ibid.* **408**, 285 (1933).
[17] J. Lindhard, K. Dan. Vidensk. Selsk. Mat. Fys. Medd. **28**, 1 (1954).
[18] J. Lindhard and A. Winther, K. Dan. Vidensk. Selsk. Mat. Fys. Medd. **34**, 1 (1964).
[19] N. D. Mermin, Phys. Rev. B **1**, 2362 (1970).
[20] A. K. Das, J. Phys. F: Met. Phys. **5**, 2035 (1975).
[21] H. B. Nersisyan, A. K. Das, and H. H. Matevosyan, Phys. Rev. E **66**, 046415 (2002).
[22] H. B. Nersisyan and A. K. Das, Nucl. Instrum. Methods Phys. Res. B **205**, 281 (2003).
[23] H. B. Nersisyan and A. K. Das, Phys. Rev. E **69**, 046404 (2004).
[24] H. B. Nersisyan and A. K. Das, in *Advances in Plasma Physics Researches*, edited by F. Gerard (Nova Science, New York, 2008), Vol. 6, Chap. 2, p. 81.
[25] J. C. Ashley, Nucl. Instrum. Methods **170**, 197 (1980).
[26] Y. N. Wang and T. C. Ma, Nucl. Instrum. Methods Phys. Res. B **51**, 216 (1990).
[27] T. C. Ma, Y. N. Wang, and T. Cui, J. Appl. Phys. **72**, 3838 (1992).
[28] G. F. Giuliani and J. J. Quinn, Phys. Rev. B **29**, 2321 (1984).
[29] D. J. W. Geldart, A. K. Das, and G. Gumbs, Solid State Commun. **60**, 987 (1986).
[30] J. G. Cordes and A. K. Das, Solid State Commun. **80**, 145 (1991).
[31] F. Stern, Phys. Rev. Lett. **18**, 546 (1967).
[32] J. H. Davies, *The Physics of Low-Dimensional Semiconductors* (Cambridge University Press, Cambridge, England, 1998).
[33] T. Ando, A. B. Fowler, and F. Stern, Rev. Mod. Phys. **54**, 437 (1982).
[34] I. S. Gradshteyn and I. M. Ryzhik, *Table of Integrals, Series and Products* (Academic, New York, 1980).
[35] A. Gold and L. Calmels, Phys. Rev. B **48**, 11622 (1993).
[36] A. L. Fetter, Ann. Phys. **81**, 367 (1973).
[37] R. A. Ferrell, Phys. Rev. **111**, 1214 (1958).
[38] G. Zwicknagel, C. Toepffer, and P.-G. Reinhard, Phys. Rep. **309**, 117 (1999).
[39] H. B. Nersisyan and A. K. Das, Phys. Lett. A **296**, 131 (2002).
[40] S. P. Møller, A. Csete, T. Ichioka, H. Knudsen, U. I. Uggerhøj, and H. H. Andersen, Phys. Rev. Lett. **88**, 193201 (2002).
[41] K. S. Singwi and M. P. Tosi, Solid State Phys. **36**, 177 (1981); S. Ichimaru, Rev. Mod. Phys. **54**, 1017 (1982).
[42] K. J. Hameeuw, F. Brosens, and J. T. Devreese, Eur. Phys. J. B **35**, 93 (2003).
[43] H. B. Nersisyan and A. K. Das, Phys. Rev. E **62**, 5636 (2000).
[44] Th. Peter and J. Meyer-ter-Vehn, Phys. Rev. A **43**, 1998 (1991).
[45] K. Morawetz and U. Fuhrmann, Phys. Rev. E **61**, 2272 (2000); **62**, 4382 (2000).
[46] G. S. Atwal and N. W. Ashcroft, Phys. Rev. B **65**, 115109 (2002).